

Removing and Reducing Scalings – Practical Experience in the Operation of Geothermal Systems

¹Johannes Birner, ²Andrea Seibt, ³Torsten Hinrichs, ¹Peter Seibt, ¹Markus Wolfgramm

¹Geothermie Neubrandenburg GmbH, Postbox 11 01 20, 17041 Neubrandenburg, Germany,

²BWG Geochemische Beratung GmbH, Seestraße 7, 17033 Neubrandenburg, Germany

³Erdwärme Neustadt-Glewe GmbH, 19306 Neustadt-Glewe, Germany

Corresponding author: birner@gtn-online.de

Keywords: Inhibitor, scaling, barite, sedimentary basin, brine

ABSTRACT

North German Basin aquifers exploited for geothermal energy uses are Mesozoic sandstones, more rarely Permo-Carbon volcanites and sandstones. The thermal waters are highly saline Na(Ca)Cl solutions. Their salinity and Ca/Na ratio increase with depth. Reducing conditions and pH values ranging from 5.5 to 6.5 are typical. Secondary components are mainly heavy metals (particularly iron and lead). Scaling may form a massive problem in the operation of geothermal systems. In Germany, mainly sites with aquifer temperatures >90 °C and highly saline thermal waters are affected.

Since 1994, a geothermal plant has operated successfully in Neustadt-Glewe. However, solid precipitations were found at several locations in the thermal water loop during maintenance work and well inspections. They consisted of calcite, aragonite, and dolomite as well as heavy metal compounds such as iron hydroxides or oxides, and lead-bearing compounds (gallenite). Poorly soluble coelestine-barite solid solutions ((Ba, Sr)SO₄) were observed, mainly in heat exchangers. Although the cooled fluid passes a fine filtration unit prior to injection, a deterioration of the injectivity has been registered in recent years, which could be partly improved by periodically soft HCl acidizing.

In order to prevent further clogging of the near-well zone by poorly soluble compounds such as barite and galenite, adequate inhibitors were selected to be compatible with the rocks, fluids, and temperatures occurring in the North German Basin. These investigations are an integral part of the research project “ContraPart” (FKZ: 0325408 A), which is funded by the Federal Ministry for the Environment, Nature Conservation, Building and Nuclear Safety of Germany.

The efficiency of these inhibitors was determined in laboratory tests by means of turbidity measurements with oversaturated BaSO₄ model brines. Potential water-rock-inhibitor interactions were studied in batch tests with representative rock materials and site-typical Na-Ca-Sr-Ba-Cl-SO₄ model water at different temperatures. All tested inhibitor mixtures resulted in a reduction of the reaction rate of barium sulphate precipitation compared to tests without inhibitor. Furthermore, no negative rock-inhibitor interactions were observed.

For the very first time, adequate inhibitors were applied to avoid barite scaling in the Neustadt-Glewe geothermal plant in the North German Basin after giving due consideration to the cost, benefits, and risks involved.

1. INTRODUCTION

1.1 Scientific Problems

Neustadt-Glewe is Germany's first power plant with combined power and heat generation. Since 1995, mass fluxes of about 80-100 m³/h with temperatures of ca. 94-99 °C are pumped off the 2200 m deep Triassic “Contorta” sandstones. The reservoir fluid is characterized by a high saline NaCl brine (total dissolved solids of approximately 220 g/l). Since the beginning of operation, the thermal water has been analyzed in frequent intervals, whereas significant changes in major ion concentrations were not observed. In addition to geochemical water analyses, deposits in filters and plant components as well as solid matter that was obtained during deep sampling in the injection well were investigated. Carbonate, coelestine barite, elemental lead and lead sulfide were detected. It is suggested that the latter derive from an electrochemical provoked steel corrosion. Furthermore, the formation of coelestine barite mixed crystals is remarkable as geochemical modeling results yielded only a very slight supersaturation for barite and no supersaturation for coelestine (Schröder et al. 2007).

However, after 3 years of operation a significant decrease of the injectivity was observed in October 1998, thereby considering different production rates and cooling temperatures (Seibt et al. 2010). In order to improve the injectivity again acidizing was conducted. Therefore, hydrochloric acid was added over several hours to the injection volume flow at the drilling head (Wolfgramm et al. 2012). The acidizing was successful and led to a reestablishment of the initial conditions (“Initial 11/97”). Likewise, after the second acidizing of drilling Gt NG 2/89 was required in 2007 the initial injectivity of about 22 m³/(h*bar) was well restored. Subsequently, a continuous decrease of the injectivity index was monitored (Figure 1). In fact, an optimized concept for acidizing in 2014 resulted in an improvement compared to the injectivity in 2012, but the negative influence of acid-insoluble compounds on the injectivity remains.

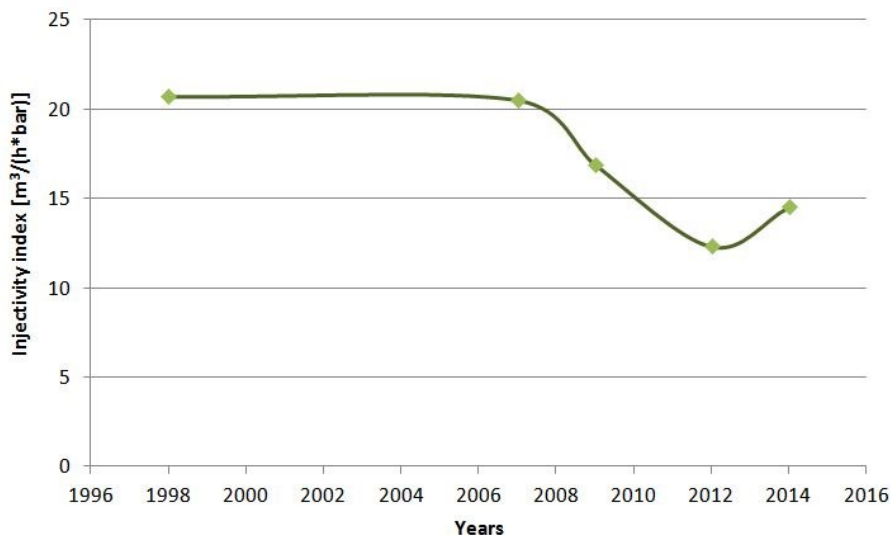


Figure 1: Development of the injectivity behaviour of drilling Gt NG 2/89 (each after acidizing)

Scale inhibitors are already used in the oil production for quite some time, especially if barium-rich formation water is injected into sulfate-rich water of petroleum reservoirs. Though manifold investigations were carried out, the interplay between inhibitors and dissolved ions like Ca, Mg and Fe in the extremely saline brines as well as at high temperatures remained unclear. Recently, the application of inhibitors in geothermal power plants has increased, whereas the conditions of use are different to those in the oil production. Therefore, the major aim of this study was to identify appropriate inhibitors, particularly in order to reduce barite scaling under the given conditions.

1.2 Efficiency of Inhibitors for Geothermal Energy

Inhibitors are substances that counteract, delay or prohibit specific reactions. In general, two different action principles exist:

1. Inhibition of crystal nucleation: Complexation of corresponding cations (e.g., Ba^{2+}) to soluble complexes
2. Reduction of crystal growth: Chemisorption at actively growing crystal surfaces (e.g., Ba^{2+} or SO_4^{2-})

In contrast to stoichiometric complexation, the effect of inhibition occurs for chemisorptions under substoichiometric conditions at the scaling that gets inhibited (threshold-effect). This leads to slower crystal growth as well as the development of a different crystal morphology. Newly built minerals typically exhibit rounder shapes. The employed concentration is generally a few mg inhibitor per Liter of fluid. Organic compounds that are ascribed so-called threshold-attributes are low-molecular polycarboxylates including polyacrylates, polymaleates and phosphonates.

The inhibitor efficiency depends on the molecule size, co-ions in the fluid, fluid temperature, pH of the solution, as well as the contact time (Miller & O'Neill 1991, Graham et al. 2003, Van der Leeden et al. 1988, Sorbie et al. 2004). As factors influencing barite precipitation in real aqueous systems are often diversified, predictions on the efficiency are hardly possible and individual selections are required for every site.

Therefore, the choice of an appropriate scale inhibitor should be based on the following criteria:

- High inhibitor efficiency at low concentrations.
- High thermal stability.
- Compatibility with formation water.
- Re-dissolution behavior to precipitated BaSO_4 -scales.
- Detectability of the inhibitor during permanent dosing into the thermal loop.

Besides hydrochemical conditions and the thermal water temperature, consequences of the inhibitors on plant components and on the aquifer rock have to be taken into account in order to select an appropriate inhibitor (respectively an inhibitor mixture). As it is common at geothermal sites to apply several different and partially also untested materials and furthermore, the conditions (hydrochemistry, pressure, temperature, volume fluxes) are usually not comparable to conditions in water treatment plants and oil industry, material compatibility should be tested prior to a long term injection of inhibitors in a geothermal power plant.

Thus, the following procedure was conducted prior to an inhibitor application in the plant:

1. Selection of substances according to efficiency, selectivity as well as chemical and thermal stability.
2. Laboratory tests with BaSO_4 model solutions and the selected inhibitors as well as inhibitor mixtures, respectively, for a comparison of the efficiency.
3. Determination of the minimal required inhibitor concentration.
4. Implementation of fluid-rock interactions (batch experiments) under real temperature conditions.
5. Long term experiments with original water and inhibitor (compatibility of materials).

2. SELECTION OF APPROPRIATE INHIBITOR

2.1 Methods

2.1.1 Applied Solutions

The following solutions were produced for laboratory experiments:

- (a) Primary salt solution: Na-Ca-Sr-Cl Sole (model solution)
- (b) Test product: Inhibitor solution
- (c) Secondary solution: $\text{BaCl}_2 \cdot 2\text{H}_2\text{O}$ and Na_2SO_4 solution

(a) 3.26 mol/L NaCl (Geyer p.a.), 0.28 mol/L $\text{CaCl}_2 \cdot 2\text{H}_2\text{O}$ (Geyer p.a.) and 5.0 mmol/L $\text{SrCl}_2 \cdot 6\text{H}_2\text{O}$ (ACS reagent grade, Merck) were used as background electrolytes. For simplifying the ion diversity in the original solution, the K-ion concentration was converted into a Na-ion concentration. Hence, one total concentration of Na was generated. Correspondingly, all bivalent ions except for strontium were converted into Ca-ion concentrations and represent a total Ca concentration. Strontium correlates with the original fluid concentration. Total dissolved solids of the model solution was 222 g/l and pH was 4.9 ($T= 20.8^\circ\text{C}$).

(b) Various commercial scale inhibitors, mainly phosphonates and one polymer in combination with phosphonate were used in this study. The selection of inhibitors arose from four inhibitor formulations that were the most promising due to extensive research and preselection. For simplification, colors were assigned to these inhibitors: BLUE, RED, PINK and BROWN. All employed concentrations that were used are active component concentrations. Therefore, a comparison of the inhibitor efficiency was possible.

(c) Diluted $\text{BaCl}_2 \cdot 2\text{H}_2\text{O}$ (ACS reagent grade, Baker) and Na_2SO_4 (Geyer p.a.) solutions were produced with regard to the reaction volume (50 ml tubes for dynamic bottle-tests and 150 ml tins for fluid-rock-interactions).

After tempering the primary solution to 60°C , the inhibitor was added, followed by the NaSO_4 solution and the BaSO_4 solution which was in accordance with the start point of the reaction.

2.1.2 Dynamic Bottle-Tests

The inhibitor efficiency tests at low-temperature (60°C) conditions were conducted by dynamic bottle-test methods. An incubator (Certomat H) was used for tempering of the tubes. Several samples can be kept in motion ($n= 125$ rpm) at once on a distributing jigger (Certomat S). Turbidity measurements, conducted with a photometer (SQ 118; Merck), were used to determine the reaction progress of the BaSO_4 precipitation. In dynamic bottle tests the first hours after dosing ($t= >6$ h) are crucial for the inhibitor application and efficiency. Measuring was carried out hourly since the start of the reaction and the reaction was aborted after 45 hours. The solution was filtered ($0.45 \mu\text{m}$) and diluted to V100 with 0.75% HNO_3 . Residual concentrations of the barium and strontium were measured with ICP-MS. In order to determine particle size and crystal morphology, solid matter analyses of the filtrate were conducted with SEM-EDX.

2.1.3 Batch Experiments

As previously described, all three solutions (a, b and c) were added to finely ground rock material. In contrast to the dynamic bottle-tests, this test series was carried out with the original concentration (test series N-A) and an exaggerated concentration of barium and sulfate (test series N-B). The relation between solid matter and solution accounts to 1:15. Preliminary tests were conducted according to the conditions at the Neustadt-Glewe power plant with a temperature of 60°C and 100°C but under atmospheric pressure. The solid matter is a quartz-rich "Contorta" sandstone from the drilling Neuruppin Gt Nn 2/87 that was extracted at a depth of 2344 m and coincides with the deltaic "Contorta" sandstones at Neustadt-Glewe.

Internal coated, airtight tin plates were used as reaction vessels (composition from inside to outside: $\text{FeSn}_2 \dots \text{Sn} \dots \text{SnO}$ or $\text{Sn}(\text{OH})_2 \dots$ oil film/paint). For each test series 25 reaction vessels were filled simultaneously. This was equivalent to 5 samples per inhibitor and one reference sample without inhibitor.

Sampling was conducted in both test series at $T= 60^\circ\text{C}$ after 2, 6, 24, 72 and 168 hours and at $T= 100^\circ\text{C}$ after 3, 6, 24, 72 and 168 hours. Therefore, the tins were opened and a sample was extracted from the fluid phase for chemical analysis. Lead, strontium and sulfate concentrations were measured to make statements on the barite kinetics. Further, potassium and aluminium concentrations were analyzed in order to describe the inhibitor-rock interactions. Subsequently, a representative solid matter subsample was taken and filtered with a $0.45 \mu\text{m}$ cellulose acetate filter. The sample was dried at ambient temperature for microscopic analysis.

2.2 Results

2.2.1 Preliminary Tests

As barium and sulfate concentrations in the Neustadt-Glewe fluid are extremely low ($c_{\text{Ba}}= 6.5 \text{ mg/l}$ and $c_{\text{SO}_4}= 440 \text{ mg/l}$), it was necessary to optimize the exaggeration of the concentration which allows for a contemporary measurement of the barium-sulfate precipitation progress. The mol ratio $n_{\text{Ba}}/n_{\text{SO}_4}= 0.01$ was kept constant while determining the precipitation velocity of different concentration exaggerations (Figure 2). With increasing extinction, more solid matter is generated whereupon a possible formation of Ba-Sr-mixed crystals is detected during the turbidity measurement as well. Up to a 3-fold and from a 5.5-fold exaggeration, respectively, tracing the reaction was not possible due to either a delayed or an instantaneous barite precipitation. Further tests were carried out with an initial barium concentration of 25 mg/l.

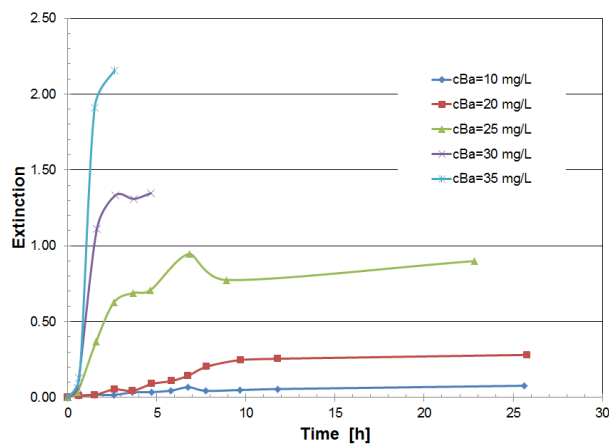


Figure 2: Chronological sequence of the extinction of thermodynamically supersaturated BaSO_4 solutions in a Na-Ca-Sr-Cl-matrix (TDS= 222 g/l), $T= 60$ °C.

2.2.2 Inhibition-Efficiency Test

The four inhibitors (BLUE, RED, PINK and BROWN) were analyzed for two concentrations. Denoted inhibitor concentrations of the test series N-A (5 mg/l) and N-B (15 mg/l), respectively, always referring to the active concentrations. As differences in the results between the two concentrations are minor, only the analysis for a concentration of $c= 5$ mg/l is shown in figure 3 (left). Here, the extinction of the inhibitors depending on the reaction time is compared with the blind sample without inhibitor. The data similarity of the reference sample without inhibitor for both test series N-A and N-B suggests an accurate reproducibility and confirms the selection of the turbidity measurements for tracing the reaction progress. Within 6 hours a significant solid matter formation was recognized, reflecting the increase of the extinction. After 45 hours reaction time, a residual Ba and Sr concentration of 6.9 mg/l and 415 mg/l, respectively, was detected by chemical analysis (analysis error of Ba: about 2.5 % and Sr: about 1.6 %). In contrast, the curve progressions of the samples with tested inhibitors show a strong reduction of barium and barium-strontium precipitation. In order to identify marginal variations between the inhibitors, the y-axis scaling was limited to 0.10 in figure 3 (right). Between the tested inhibitors, almost no differences were observable in the precipitation behavior during the observation period. Overall, only little solid matter was formed. After a maximum extinction value was reached, the value decreased again and persisted more or less constant until the reaction is aborted. It is suggested, that an alteration of the crystal structure occurs. Only a minor decrease of barium was observed analytically, independent from the active concentration of the inhibitor. Strontium concentrations decreased about 30 mg/l. A concentration increase had no additional effect. A first tendency with respect to the efficiency was reached for an inhibitor active concentration of 5 mg/l: BLUE>RED>BROWN>PINK.

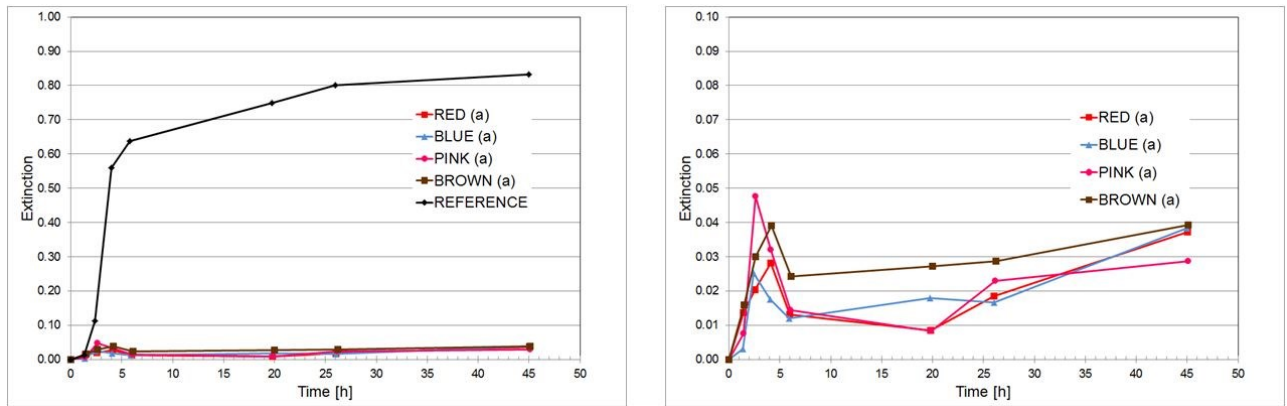


Figure 3: left: Extinction depending on the reaction time, Ba initial concentration of 25 mg/l at $T= 60$ °C (± 0.5 °C) and a shaking velocity of 125 rpm (inhibitor RED, BLUE, PINK and BROWN for $c= 5$ mg/l (A) in comparison to the reference sample without inhibitor); right: Zoomed view on extinction against reaction time only for the inhibitors.

The solid matter of the test series was analyzed with respect to amount, size and habitus of the barites as well as possible phosphate precipitations. Amount and size of the barite crystals were measured by a scanning electron micrograph (SEM) with backscatter electron detector (BSE) at 100-fold magnification. Thereafter, the representative overview screens were analyzed via digital image data analyses according to Anselmetti et al. (1998). The particle size was simplified and calculated as the square root of the particle area. Statements on the crystal habitus are based on BSE-images with 800-fold to 1000-fold magnification. The barite crystals are distinguishable in the pictures due to their high density. As heavy elements lead to a strong back scattering, those areas appear pale. In contrast, areas with lighter elements appear darker. A relatively tight selection spectrum was applied for the digital picture data analysis in order to consider ray diffusion at the borders of the lighter particles during back scattering of electrons. Additionally, the chemical composition of the lighter and darker filter areas was checked with energy dispersive x-ray analysis (EDX) previous to the digital picture data analysis to assure that barites are actually represented by lighter particles. During this screening, the fine grained matrix composition was analyzed as well to detect possible phosphate precipitation.

Figure 4 shows the used image sections and the barite portion of these sections. Without applying inhibitors (blind sample) plenty of barite crystals form after a short time period and cover 8.4 % of the total filter area. In contrast, the application of inhibitors leads to a decrease of barite precipitation for all samples of more than 88 %. The highest efficiency was observed for the inhibitor RED with only 0.1 % filter area coating that leads to a 98.8 % reduction of barite precipitation. The effect of the inhibitors BLUE and PINK are excellent compared to the blind sample. However, their efficiency of barite reduction between 88 and 89 % lags significantly behind that of the RED inhibitor. The BROWN inhibitor is characterized by an above-average efficiency for the inhibition of BaSO_4 with a filter coating of 0.6 % that implies a reduction of barite precipitation of 92.8 %.

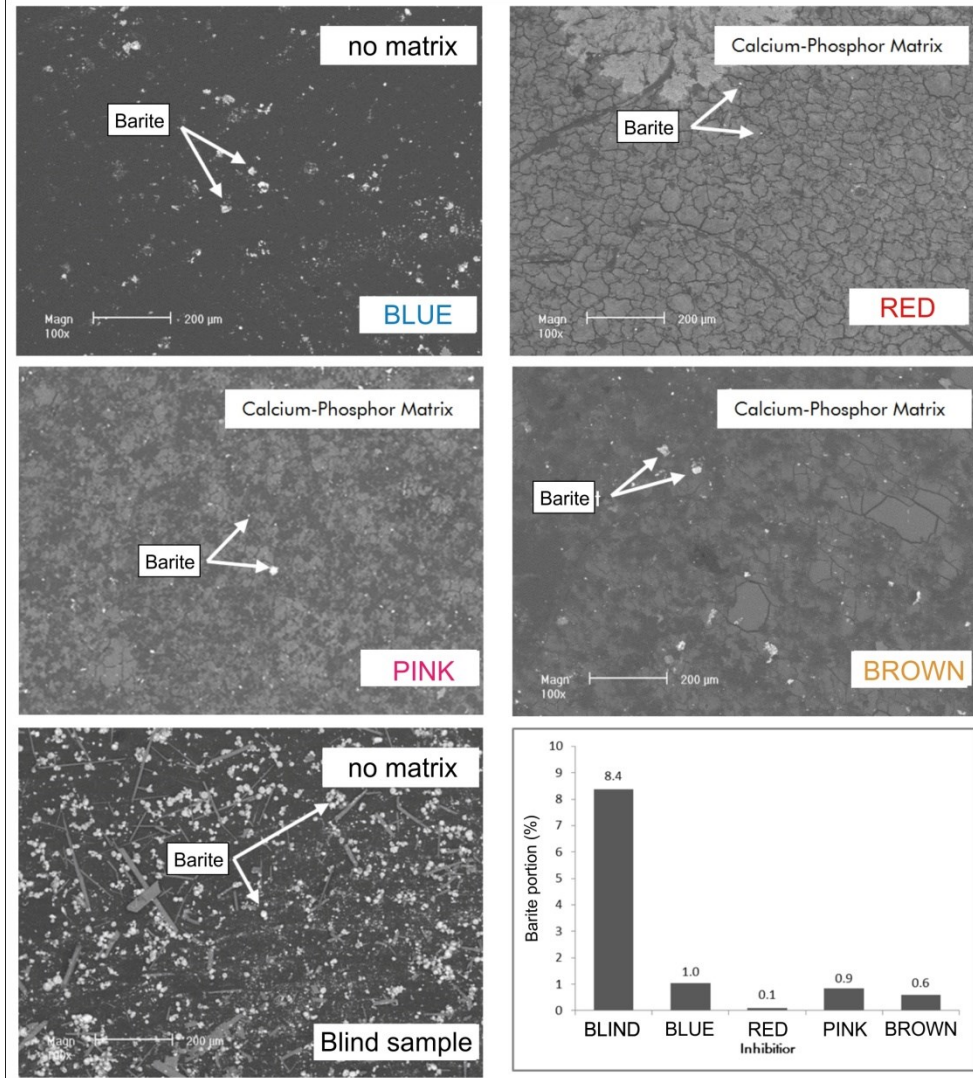


Figure 4: SEM images at 100-fold magnification and BSE-detector of the blind sample and the inhibitors BLUE, RED, PINK and BROWN. The diagram shows the barite portion of the total analyzed image area

The application of inhibitors led to a decrease of the mean barite crystal particle size (Figure 4). This effect was already indicated during the analysis of the maximum size. Without inhibitor, the maximum size was 33.2 μm , while for the BLUE inhibitor it reduced to 25.5 μm . Furthermore, the maximum size was reduced to 24.2 μm for the BROWN inhibitor and to 20.0 μm for the PINK inhibitor. Most prominent was the impact of inhibitor application related to the crystal growth for the RED inhibitor with a maximal particle size of only 7.8 μm . An analysis of the grain size distribution confirmed this trend. Here, 35 % of all particles exhibited a size $>5 \mu\text{m}$ without inhibitor application. Contrary, the inhibitor BLUE led to a reduction of 17.8 % for big particles $>5 \mu\text{m}$, BROWN reduced the particle size $>5 \mu\text{m}$ to 13.5 % and RED as well as PINK to 7 %.

The influence of the applied inhibitors on the barite crystal habitus is presented in figure 5. While idiomorphic, radiating barite minerals can form in the blind sample without inhibitor, the application of inhibitors constrains the crystal growth. Idiomorphic crystals were not observed in samples with inhibitor which may be attributed to the small size of barites. All larger barite crystals indicate the significant influence of inhibitors on the crystal habitus. For inhibitor BLUE, mainly small and spherical minerals with relatively smooth surfaces formed. The application of inhibitor RED causes the generation of tiny, fibrous barite crystals that resemble the singular radiating fibers developing without inhibitor. Here, a crystal structure was not recognized. The barite morphology for solutions with the inhibitors PINK and BROWN were similar. They consisted of a porous and untextured material accumulation.

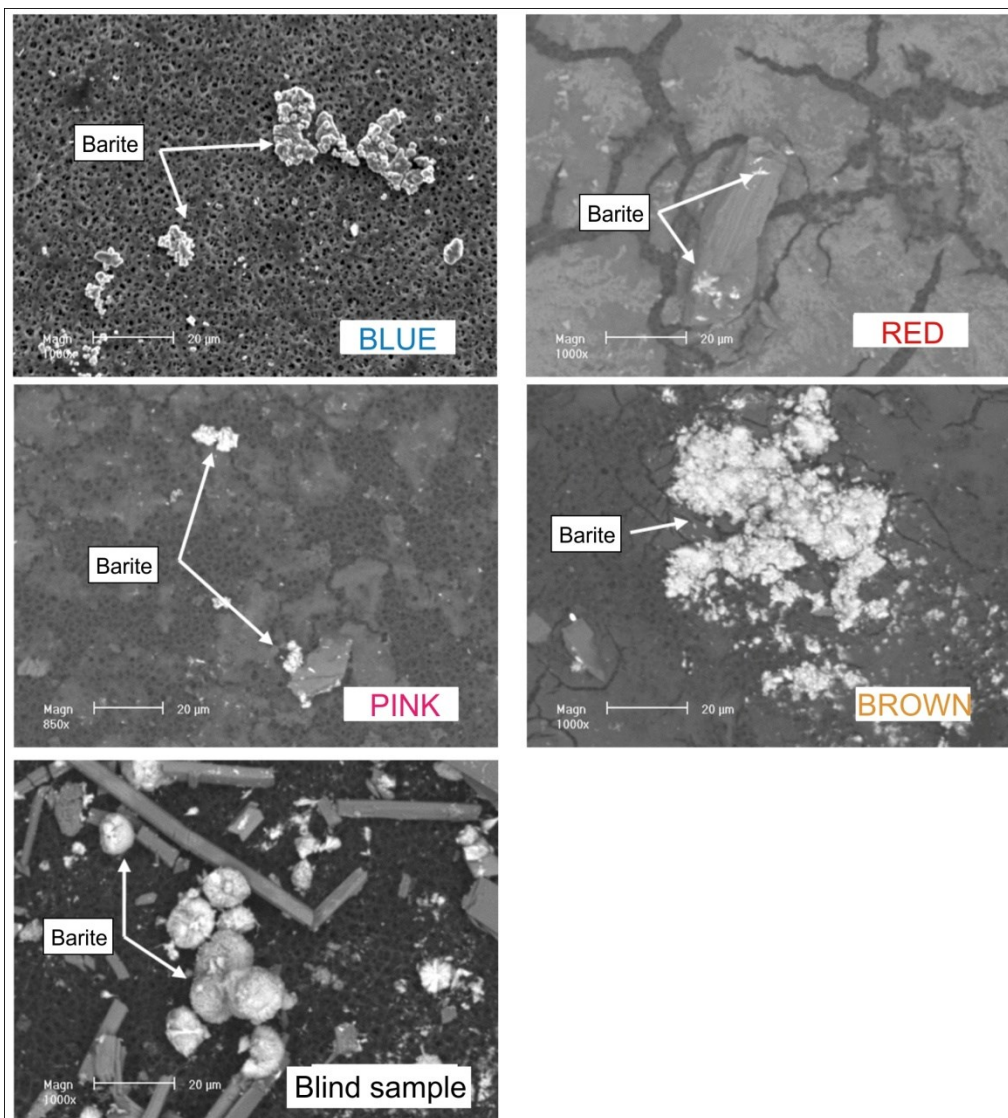


Figure 5: SEM images at 850- to 1000-fold magnification and BSE-detector of the blind sample and the inhibitors BLUE, RED, PINK and BROWN for the determination of the barite precipitation morphology.

It is apparent from figure 4, that the filters of the samples RED, PINK and BROWN was coated with a very fine matrix which was identified by EDX-analysis as a calcium-phosphorous bond. This suggests that the inhibitors RED, PINK and BROWN led to a precipitation of very fine grained phosphate at an active concentration of 15 mg/l. These precipitations must not occur during system operation. In order to investigate the behavior of inhibitors under realistic concentrations, the filter with an active concentration of 5 mg/l was used. The results showed no fine grained matrix in any of the samples and also the EDX-analysis did not give evidence on phosphate precipitation. Thus, there was no risk of unrequested phosphate precipitation for active concentrations <5 mg/l.

2.2.3 Batch Experiments

The reaction kinetics during batch experiments with exaggerated BaSO_4 concentrations illustrate the efficiency of inhibitors concerning a slowdown or prevention of barium (-strontium) sulfate and barium sulfide precipitation. Due to the exaggeration in batch experiments, the efficiency of the inhibitor is more visible and easier to quantify. Figure 6 presents the barium concentrations in the fluid during test series N-B (exaggerated BaSO_4 concentration) at a temperature of $T= 60^\circ\text{C}$. As a result of the exaggerated concentrations, barium minerals precipitate fast. The concentration without addition of inhibitors (blind sample) increased about 45 % within 2 hours. Four hours later, a further 21 % increase was observed and one day after beginning of the experiment additional 23 %. Overall, a decrease from about 25 mg/l to concentrations of 0.0063 mg/l was observed. At the end of the experiment only 1 % of the initial concentration remained dissolved. The repressive effect of the inhibitors for the barium mineral precipitation can be demonstrated if comparing solution contents with and without inhibitor. After 2 hours, all samples with inhibitor showed significantly higher barium concentrations in solution. Especially for the inhibitors BROWN, RED and BLUE, barium concentrations in solution are 20-30 % larger than the barium concentration without inhibitor. Regarding barium concentrations after one week, the repressive effect was intensified for low concentrations. While without inhibitor only 0.063 mg/l barium remained in solution, barium concentrations with inhibitor were many times higher (BLUE: 0.178 mg/l; RED: 0.304 mg/l; PINK: 0.234 mg/l; BROWN: 0.236 mg/l). Additionally, for the test series N-A (with aquifer typical BaSO_4 concentration), all inhibitors led to higher barium concentrations in solution as would be the case without inhibitor although the effect was less pronounced in this test series.

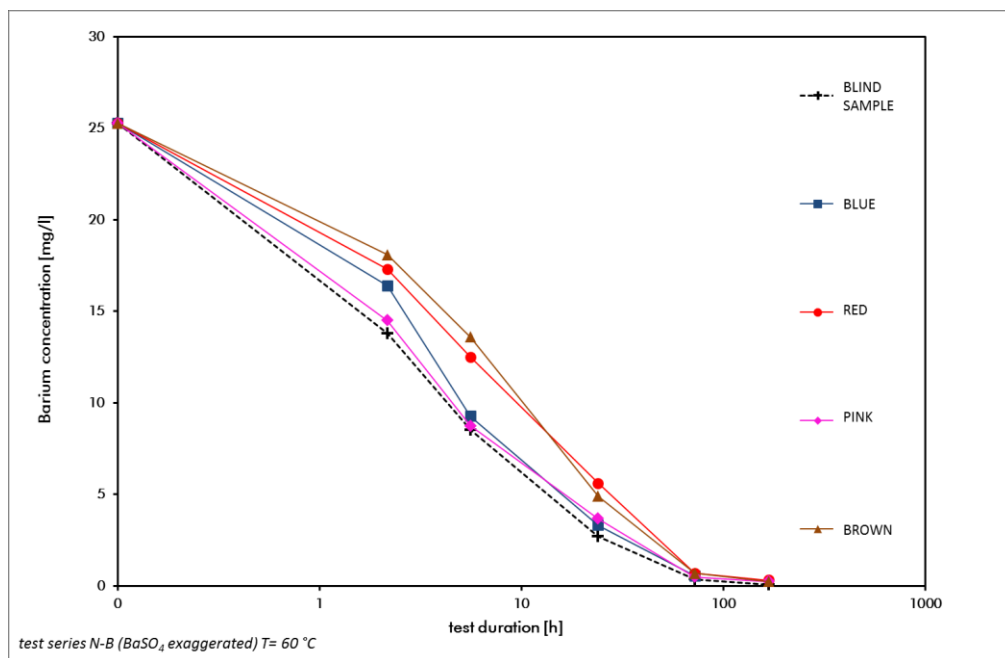


Figure 6: Barium concentrations of the test series N-B (exaggerated BaSO_4 concentration) at a temperature of $T= 60\text{ }^{\circ}\text{C}$ during the batch experiment.

Finally, the used rock samples were tested for corrosion as a result of the applied inhibitors. Here, as well as for the analyses of potassium and aluminium concentrations that indicate silica decay, no differences were observed between samples with and without inhibitor. This leads to the conclusion that the applied inhibitors do not cause rock corrosion.

2.3 Evaluation and Selection of an Inhibitor for Application in the Geothermal Power Plant Neustadt-Glewe

The major aim of the laboratory experiments was to select an appropriate inhibitor for an application in the geothermal power plant Neustadt-Glewe in order to prohibit barium sulfate precipitations. Therefore, the investigated inhibitors were evaluated regarding their efficiency and ability on a scale from 1 ('very good') to 5 ('unsatisfactory'). In conclusion, the inhibitor BLUE provided for all experiments the best results and was marked with 1 ('very good'). In second place came the inhibitors RED and BROWN with an overall grade of 1.9 ('good'). Both were 'very good' in some experiments but yielded only 'satisfactory' results in other tests. For example, BROWN was among the best inhibitors in the closed-bottle test and the batch experiments but lagged behind the others in the turbidity measurements. Overall, both may be considered as an alternative to the BLUE inhibitor. The PINK inhibitor received the overall grade of 2.5 ('still good'), due to its average behavior in almost all experiments.

Besides the pure effect of the inhibitor, crucial factors for the right inhibitor selection include aspects like thermal stability, biodegradability and the on-site manageability. For example, the inhibitor RED had to be diluted prior to an injection into the original fluid. Otherwise, instantaneous salification occurs as shown with the calcium tolerance test. The inhibitor RED should only be applied as ready-made diluted product in order to avoid the need for dilution of the inhibitor on-site.

3. PILOT TEST: INHIBITOR APPLICATION IN A GEOTHERMAL POWER PLANT

In spite of an accurate inhibitor application supported by extensive preliminary laboratory experiments, interferences by additional solid matter precipitation and corrosion of plant components may occur in a geothermal power plant. Therefore, the experimental application in the thermal water cycle in April 2014 was accompanied by an adjusted monitoring program. In addition to a controlling of solid matter in the thermal water cycle by fine filtration, hydrochemical monitoring was conducted. Due to the operation mode ($Q= 62\text{ m}^3/\text{h}$), it was not possible to measure an injection pressure.

Solid matter was analyzed for a reduction of crystal growth due to adsorption of the inhibitor at actively growing crystal surfaces as well as for the formation of unrequested byproducts. The screening of coarse and fine particle loads was concentrated on the section in the thermal water cycle, where the inhibitor flows through. The first fine filtration for an analysis of the particle load was conducted at a sampling tap located behind the heat exchange device which was about 25 m rearward the inhibitor injection point. The second filtration was carried out directly ahead the fine filters at the injection well (figure 7). It has to be considered that for any variation of the inhibitor concentration (active concentration) the monitoring must be repeated.

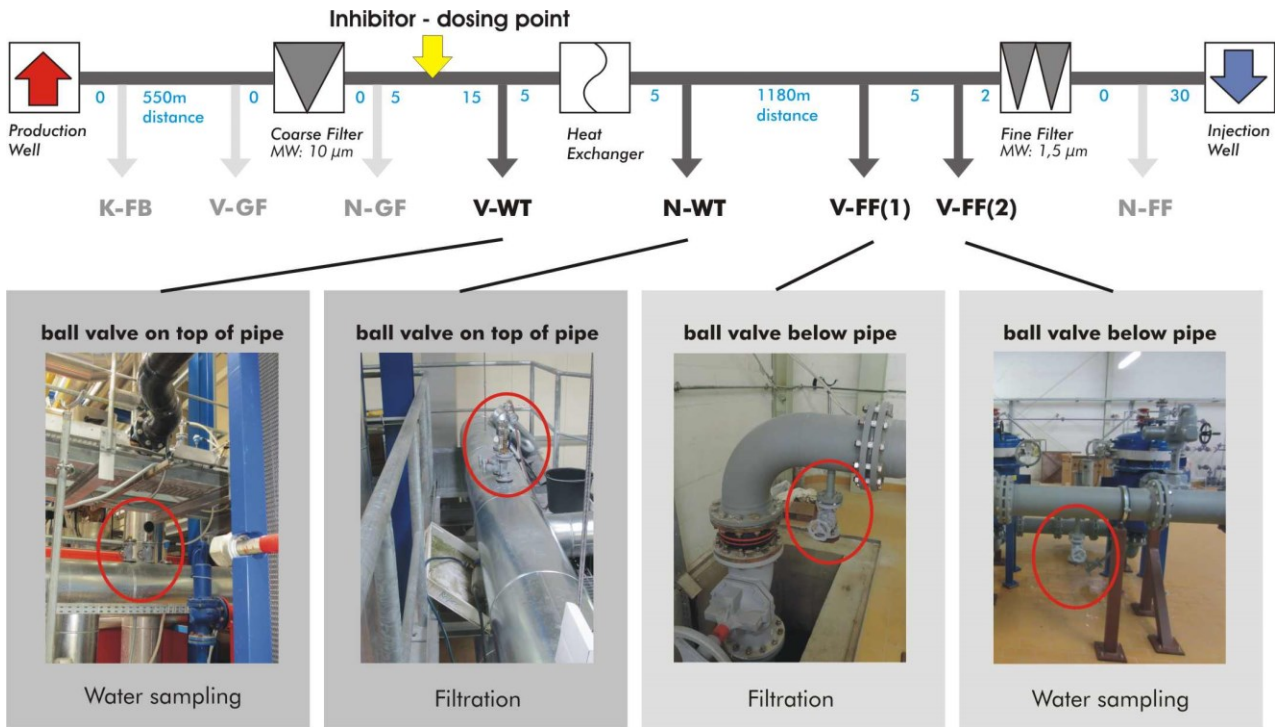


Figure 7: Filter and sampling locations of the monitoring program during inhibitor application; the yellow arrow marks the position for an inhibitor injection.

3.1 Installation

The inhibitor injection point was chosen according to the precondition that the inhibitor be completely mixed with the thermal water prior to the inflow into the heat exchanger. The input was carried out with a dosing pump through an injection lance which placed the inhibitor centered in the thermal water flow. Storage of the inhibitor and installation of the dosing pump were located in the boiler house. Here, appropriate protection measures for the staff and the technical equipment were installed. For technical reasons, the lance was inserted in a part of the pipe outside the boiler house. Lance and dosing pump were connected via a 15 m long flexible stainless steel tube (figure 8).

3.2 First Application

The inhibitor BLUE with an active concentration of 3 % was chosen for the pilot test. At a temperature of $T= 20^{\circ}\text{C}$, this was equivalent to an added inhibitor amount of about 5 ml/min and a thermal water flow of 62 m³/h. The inhibitor was added to the system over 2 hours during the first application. The inserted inhibitor volume was measured with a graduated cylinder. Overall, about 639 ml inhibitor was dosed into the thermal water system in 120 min, which corresponds to a mean feeding rate of 5.3 ml/min.

Furthermore, just a limited sampling at the sampling locations ahead and behind the heat exchanger was possible due to gas present in the piping in this section of the thermal water cycle. The only available sampling taps were situated at the top side of the pipes. Despite a gas release over more than 15 minutes, no constant water flow was realizable at these taps. The volume flow ahead the heat exchanger, which was fed to the in situ parameter determination via a sampling cooler, remained little (<5 ml/min) throughout the entire time of the experiment. As a result, it was not possible to ascertain the in situ parameters in a flow-through cell, but only provisionally in a 100 ml beaker glass. Therefore, a measurement of the redox potential as well as the electrical conductivity was abandoned. Additionally, the pH was increased significantly, due to the unavoidable degassing of CO₂ in this open system. The inhibitor dosing had no significant effect on the pH value. Merely at the beginning, a slight decrease of pH by about 0.2 was observed. Contrary, at the sampling location ahead of the injection well, a slight pH increase was monitored which was attributed to the strong acidizing effect of the inhibitor. However, this implies an excellent inhibitor mixing with the thermal water and a potentially non-corrosive behavior. It can be concluded that the inhibitor application had no significant influence on the pH value of the thermal water.

Water samples were extracted at the injection well previous to the inhibitor application on 2014-03-27 and during the inhibitor dosing on 2014-04-10. The following cations were analyzed: Li, Na, K, Mg, Ba, Ca, Sr, Fe, Mn, NH₄. Further, the trace elements Al, Cr, Cu, Zn, Ni, As (total), Cd, Hg, Pb, B and Si as well as the anions Cl, SO₄, Br, F, I and PO₄ (total) and ortho-phosphate were determined. In order to avoid the effect of reaction kinetics between sampling and analytics, a dilution V100 with 0.75% HNO₃ was produced immediately after sampling for the elements Ba, Sr and SO₄. While the major cations (Ca as well) and anions remained unaffected, the Ba, Sr and SO₄ concentration, under consideration of the analysis error, decreased significantly. A reduction of 0.4 mg/l Ba and 80 mg/l Sr in solution was detected. Concentrations of the analyzed P-bonds were <0.1 mg/l. For all further elements like Fe, Mn and Pb, no changes in the concentrations were observed. Due to the very short inhibitor application, conclusions cannot be drawn yet.



Figure 8: Installations for the inhibitor injection.

As already described above, sampling downstream of the heat exchanger was strongly affected by the high gas present in the piping at these locations as well as by the position of the sampling tap at the upper side of the pipe. However, two representative solid matter samples could be filtered out by cellulose acetate filters (CAF) with a mesh size of 0.45 μm and 3 μm . As the fine filter sample with 0.45 μm was entirely coated with a fine grained matrix, the filter with a 3 μm mesh size was characterized by only a few large particles on the uncoated filter fibers (figure 9). These large particles, that were detected at the 0.45 μm sample as well, were calcites, which spontaneously formed during sampling due to the degassing of CO_2 (figure 9A, no:2). The degassing results from the pressure minimum of the power plant that was located behind the heat exchanger and was in line with the significantly increased pH values of the in situ parameter measurements at this location. SEM images as well as EDX overview spectra, where increased calcium concentrations (10-20 %) were only observed in image sections with large calcites, confirm that the particles are coarse. Both right EDX-spectra in figure 10 represent image sections without identifiable particles (figure 9D). Consequently, the calcium portion is low (2 %).

By comparing fine with coarse grained samples, it became apparent that the majority of the solid matter in the thermal water had a diameter of $<3 \mu\text{m}$ at this location. However, it had to be taken into account that the release of fine material was favored due to the position of the sampling tap at the upper side of the pipe. In the fine material ($<3 \mu\text{m}$), silica and iron concentrations were significantly increased.

Phosphorous served as an indicator for the dosed inhibitor and was detected both at the fine and the coarse filter sample. Concentrations of both samples (15-17 Atom-%) do not differ significantly except for those EDX spectra, which were based on analyses of filter sections without identifiable particles (figure 10, right). Here, increased phosphorous concentrations were detected ($>20 \text{ Atom-}\%$). Phosphorous appeared in comparable concentrations, on samples with a lot of fine grained material and in sections without identifiable solid material. This points to the assumption, that phosphorus coats the particles/filter fibers as a thin coating (thickness $<0.45 \mu\text{m}$) which prohibits crystal growth instead of accumulating in particles. A negative effect due to the formation of unrequested byproducts (phosphorous bearing particles) was not observed.

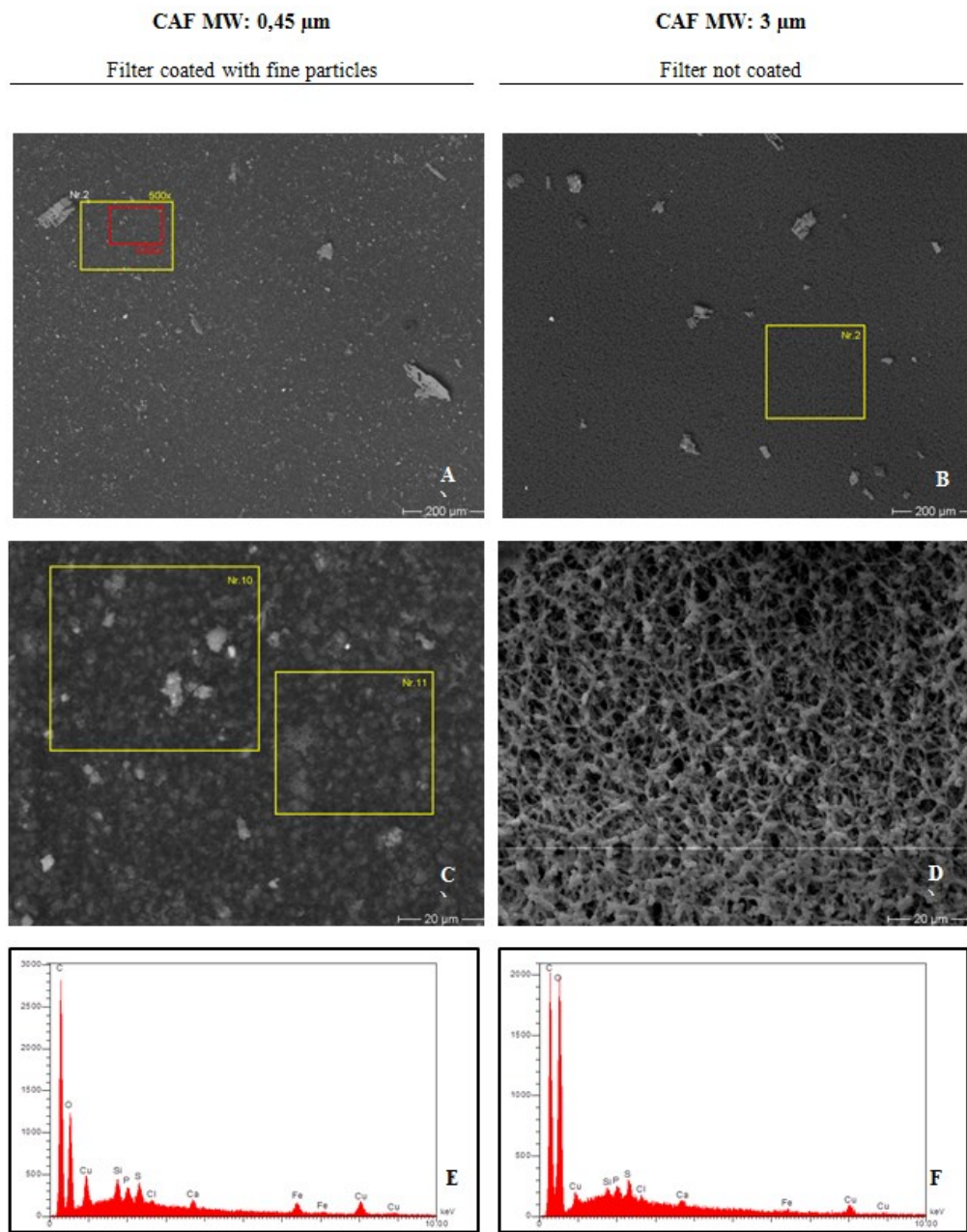


Figure 9: SEM images of the solid matter samples behind the heat exchanger (N-WT); A) 0.45 μm sample (100x): EDX image areas; B) 3 μm sample (100x): EDX image areas; C) 0.45 μm sample (100x): filter totally coated with fine grained material; D) 3 μm sample (100x): filter fibres without particle; E) 0.45 μm sample: typical EDX spectrum (compare C-no.10); F) 3 μm sample: EDX spectrum without identifiable particles (compare D).

3.3 Further Procedure

Prior to a continuous inhibitor injection it must now be verified whether or not the selected substance leads to a) a corrosion of plant components or b) a change of the mechanic characteristics of the used seals in the thermal water cycle. At the moment, a material testing of the heat exchanger discs and of the EPDM-seals is being conducted in the laboratory. After finishing the investigations on the compatibility of materials, the inhibitor will be added to the plant over a longer period of time from beginning of the heating period in autumn 2014. This inhibitor application will also be extensively monitored. The long-term investigations will focus on the analysis of the temporal injection pressure development and the filter residues.

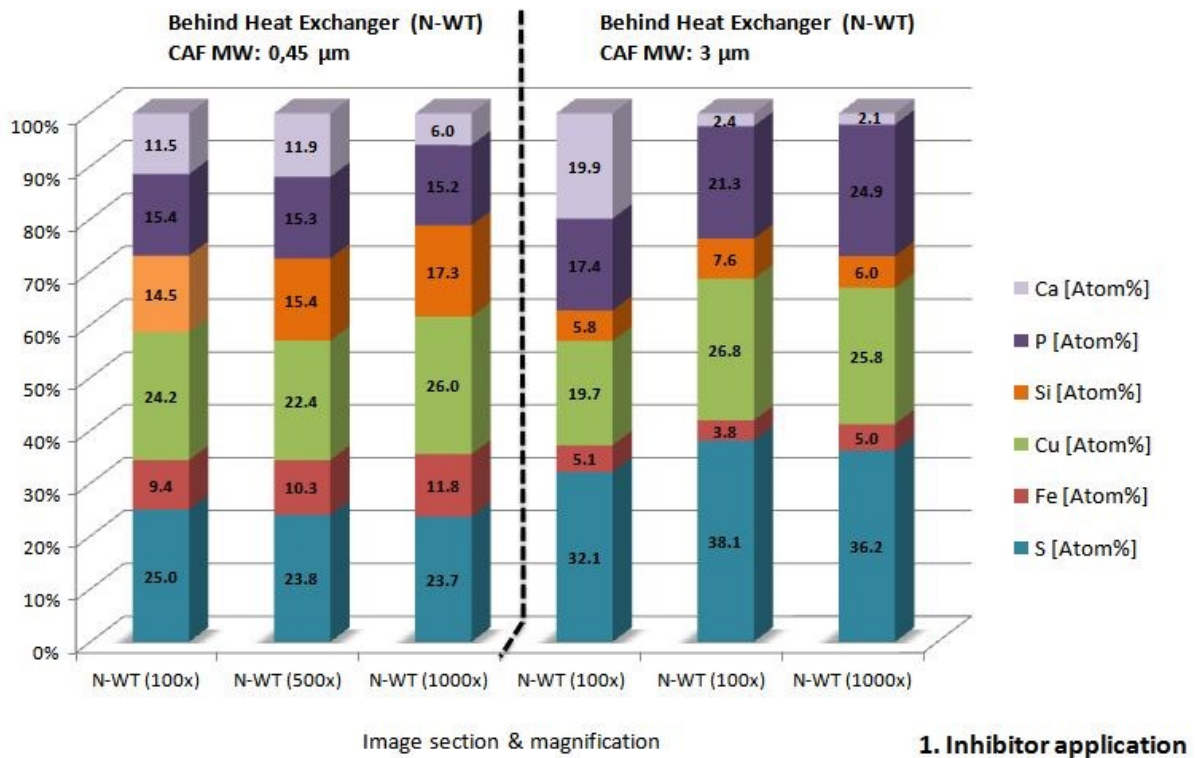


Figure 10: Analysis of EDX overview spectra of the samples behind the heat exchanger. Both spectra to the right (N-WT 100x, N-WT 1000x) represent filter sections without identifiable particles.

4. CONCLUSIONS

The aim of this work was the development of strategies to prevent negative particle effects on the thermal water cycle of geothermal power plants in the North German Basin. A particular challenge was to prohibit barium sulfate precipitations in those thermal waters, as they lead to an irreversible decrease of the injectivity. One potential measure towards a decrease of scaling was the applications of inhibitors. In this study, appropriate inhibitors were selected for the reduction of barium sulfate precipitations which were tested in the laboratory for efficiency, effectivity and inhibitor-rock interactions.

At first, preliminary experiments were carried out to determine barium and sulfate ion concentrations while keeping the geogenic mole ratio constant. This allowed for a contemporary measurement of the barium sulfate precipitation reaction progress. Subsequently, four inhibitors (BLUE, RED, PINK, BROWN) in two concentrations each (5 mg/l and 15 mg/l) were investigated in inhibition-efficiency tests. Turbidity measurements have shown that all inhibitors significantly reduced solid matter formation. During the observation period, hardly any differences in the precipitation behavior of the tested inhibitors were observed. Overall, only little solid matter formed. Microscopic investigations of the solid matter indicated an influence of the inhibitors on the crystal growth. While idiomorphic and radiating barite minerals form in the blind sample without inhibitor, the application of inhibitors constrained the crystal growth and significantly less barium sulfates with smaller diameters formed. The inhibitor efficiency was investigated on the basis of reaction kinetics in batch experiments with aquifer material and in model solutions with geogenic and exaggerated BaSO₄ concentrations, related to a delay or prevention, respectively, of barium(strontium) sulfate precipitations. After 2 hours, all samples with inhibitor showed higher barium concentrations in solution than the blind sample. Considering the barium concentrations after one week, it became apparent that the inhibiting effect was amplified for low concentrations. In addition, the test series with typical aquifer BaSO₄ concentrations indicated an increase of the barium concentration for all samples with inhibitors in contrast to those without inhibitor, even though the effect was less pronounced in this case. Finally, the rock material applied in the batch experiments was investigated for rock corrosion due to the inhibitor dosing. Here, as well as for the water analyses of potassium and aluminium concentrations that indicated silica decay, no differences were observed between samples with and without inhibitor. This led to the conclusion that the applied inhibitors do not cause rock corrosion.

On the basis of an evaluation matrix the inhibitor BLUE was selected for a first pilot test in the geothermal power plant Neustadt-Glewe. In this first field use, the inhibitor was dosed to the thermal water cycle ahead of the heat exchanger with a concentration of 3 % over two hours. Results of the inhibitor application indicated no negative changes of the water chemistry as well as no further particle formation. After finishing investigations on the compatibility of materials, further in situ investigations that focus on the efficiency and thermal stability of the inhibitors under real conditions will be conducted.

ACKNOWLEDGEMENTS

The presented investigations were carried out within the framework of the joint research project "Strategies to prevent negative particle effects on the thermal water cycle of geothermal power plants in the North German Basin and the Upper Rhine Rift

(ContraPart FKZ: 0325408 A)" supported by the Federal Ministry for the Environment, Nature Conservation, Building and Nuclear Safety (BMUB).

The authors wish to thank the staff members of Erdwärme Neustadt-Glewe GmbH for their kind support and their confidence.

REFERENCES

Anselmetti, F. S., Luthi, S. & Eberli, G. P. (1998): Quantitative characterization of carbonate pore systems by image analysis. - Am. Ass. Petr. Geol. Bull., 82, pp. 1815-1836.

Miller, J. W., O'Neil, J. J. (1991): Structure/Performance relationships for Barium Sulfate and Strontium Sulfate antiscalants. - SPE Latin American Petroleum Engineering Conference, 8-11 March, Caracas, Venezuela, p. 24

Seibt, P., Kabus, F., Wolfgramm, M., Bartels, J., Seibt, A.: Monitoring of hydrogeothermal plants in Germany – an Overview. Proceedings WGC 2010, Bali, Indonesia, 25 – 29.4.2010, 2410 (2010): 1 – 7.

Schröder, H., Teschner, M. Köhler, M., Seibt, A. Krüger, M. Friedrich, H.-J., Wolfgramm, M.: Long term reliability of geothermal plants – Examples from Germany. Proceedings European Geothermal Congress 2007 Unterhaching, Germany, 30 May-1 June 2007, 137 (2007): 1 – 7.

Sorbie, K. S., Laing, N. (2004): How scale inhibitors work: Mechanisms of selected Barium Sulphate scale inhibitors across a wide temperature range. - SPE 87470, SPE International Symposium on Oilfield Scale, 26-27 May, Aberdeen, United Kingdom, p.10.

Van Der Leeden, M. C. & Von Rosmalen, G. N. (1988): Development of inhibitor for Barium Sulphate deposition. - Proceedings intern. Symposium on Chemicals in the Oil Industry, Vol. 3, p. 65-83.

Wolfgramm, M., Birner, J., Lenz, G., Hoffmann, F., Rinke, M. (2012): Erfahrungen bei der Säurestimulation geothermaler Aquifere und Anlagen. - Proceedings of Geothermiekongress from 13.11.-16.11.2012 in Karlsruhe (Germany), F11-2: 1-12.